University of Huddersfield Repository

An, Lili, Xu, Qiang and Lu, Zhongyu

The development of advanced creep constitutive equations for high chromium steel P91 at low stress range

Original Citation

An, Lili, Xu, Qiang and Lu, Zhongyu (2013) The development of advanced creep constitutive equations for high chromium steel P91 at low stress range. In: 6th International "HIDA" Conference on Life/Defect Assessment & Failures in High Temperature Plant, 2-4 December 2013, Japan.

This version is available at http://eprints.hud.ac.uk/id/eprint/21822/

The University Repository is a digital collection of the research output of the University, available on Open Access. Copyright and Moral Rights for the items on this site are retained by the individual author and/or other copyright owners. Users may access full items free of charge; copies of full text items generally can be reproduced, displayed or performed and given to third parties in any format or medium for personal research or study, educational or not-for-profit purposes without prior permission or charge, provided:

- The authors, title and full bibliographic details is credited in any copy;
- A hyperlink and/or URL is included for the original metadata page; and
- The content is not changed in any way.

For more information, including our policy and submission procedure, please contact the Repository Team at: E.mailbox@hud.ac.uk.

http://eprints.hud.ac.uk/

The development of advanced creep constitutive equations for high chromium steel P91at low stress range

Lili An[1]; Qiang Xu[2]; Zhongyu Lu[3]

School of Computing and Engineering, University of Huddersfield, Huddersfield, UK

[1]L.An@hud.ac.uk; [2]Q.Xu2@hud.ac.uk; [3]Z.Lu@hud.ac.uk;

Corresponding author: Dr Qiang Xu, Q.Xu2@hud.ac.uk

Abstract

Diffusion dominates the creep deformation at low stress range for high chromium steel P91. Brittle creep fracture is caused by cavity nucleation, growth and coalescence of cavities and large precipitates (Laves phase and $M_{23}C_6$) at grain boundary under low stress range. At low stress range, a linear relation between strain at failure and different stresses has been described. Moreover, the minimum strain rate is also proportional to the different stresses.

The new set of constitutive equations model should describe the microstructure evolutions of $M_{23}C_6$ carbides and Laves phase, the linear relationships between strain rate and stress, strain at failure and stress. The both influence of stress and microstructural changes is regarded as the new failure criterion. Three aspects of novelty for the new set of constitutive equations model have been considered in this paper. The further work should focus on the form and validation of the new set of constitutive equations model.

Keywords: P91 steel, creep life, strain at failure, failure criterion, constitutive equations

1. Introduction

Since 1990, due to a high resistance of corrosion ability, high creep strength and the low oxidation speed of high chromium steels (9-12% Cr, particular P91 steel), high chromium steels have been widely used in power plant industries as a component of boilers, turbines, tube, pipework etc. Recently, the prediction of creep lifetime of high chromium steels becomes a serious issue, especially for weldment [1-2]. Researchers tried to predict the lifetime of materials by using creep constitutive equations models that proposed to depict the complex creep behavior within the continuum damage mechanism framework [3].

A premature failure of P91 steel has been observed during a long-term creep. The Laves phase emerges and cavities rapid coalescences during the tertiary creep stage causing a premature failure during the long-term test. The different preferential recovery mechanisms of martensite at the prior austenite grain boundary (PAGB) are homogenous and inhomogeneous recovery at high stress range and low stress range, respectively. It is argued that the premature failure is due to that inhomogeneous recovery [4].

Stress breakdown is well-known and the prediction of long term creep life (under low stress) by extrapolation from short term test (under high stress) is still of overestimated [5-10], this is due to a change of creep deformation and damage mechanisms over stress range. Most of these creep models do not consider the creep damage in details. Even the most popular creep damage constitutive model (Kachanov-Robatnov-Hayhurst, KRH), deficiencies still exist and they are primarily: 1) unable to depict the creep deformation accurately, 2) the value of υ was not able to depict the multi-axial stress state effect on creep deformation and creep damage and rupture [11-13].

An et al. [4, 14-15] has reviewed and analyzed the current experimental data of P91 steel which includes microstructural changes, creep deformation and damage mechanisms, influence of stress range on life span, influence of stress state on life span and also an analysis of the constitutive equations models [6-10,16-19]. That review identified the following main findings [5, 14-15]: 1) Dislocation creep deformation and ductile creep damage assisted by cavity nucleation, growth and coalescence process are the main features of creep deformation and damage mechanisms at high stress range; 2) By contrast, a diffusion creep deformation and a brittle creep damage caused by cavity nucleation, growth and coalescence around the grain boundary are the main features of creep deformation and damage mechanisms at low stress range; 3) The life span of materials under the multi-axial stress state is proportional to the creep stress. Also, the minimum strain rate is proportional to the creep stress [19].

This paper mainly focus on the method of development of a new set of constitutive equations model for high chromium steel P91 at low stress range. Firstly, this paper will report the cavity nucleation, growth and coalescence process at low stress range; secondly, this paper will report the diffusion-assisted brittle rupture mechanism at low stress range. Finally, this paper will report the new thoughts of developing the new set of constitutive equations model and the further work.

2. Current experiment data of P91 steel at low stress range

2.1 Microstructure evolution

2.1.1 Z-phase particles

Z-Phase particles are not considered as the reason to cause premature failure of P91 steel at low stress range. Panait [7] has reported that a few amount of modified Z-phase particles were observed after a long-term creep for 113,431h at 600°C (80MPa) for P91 material. Due to the small amount, Z-phase particles have not been considered as the reason to cause a premature failure of P91 steel at low stress range, this view was also supported by Sawada [8, 23]. Kimura and his colleagues [4, 24] also reported that the disappearance of $M_{23}C_6$ and MX type precipitates and the formation of Laves phase and Z-phase in Mod. 9Cr-1Mo steel at 600°C. The formation of Z-phase was observed after a long time creep for around 10000 hours at 600 °C. However, the formation of Laves phase was observed less than 100 hours. And then, the Laves phase starts rapidly growth and coalescence. Therefore, the few amount of Z-Phase has no significant effect to cause a premature failure for P91 steel.

2.1.2 Laves phase and $M_{23}C_6$ carbides

Laves phase and $M_{23}C_6$ carbides are regarded as the cites for cavity nucleation. Then cavity grows and coalescence contributing to and/or leading to creep damage and failure. Literature reported that only the large precipitates have a significant influence on the loss of creep strength and the attention should be focused on the large precipitates [7]. The average size of MX type precipitates is about 20-40nm. In 2010, Panait [7] also reported that there are no significant changes in size, shape and spatial distribution of MX-type precipitates. The equivalent diameter of $M_{23}C_6$ carbides is about 150nm in the as-received test pieces. After a long-term creep, the equivalent diameter of $M_{23}C_6$ carbides increases up to 300nm. The $M_{23}C_6$ carbides and MX type precipitates nucleate and grow during tempering; only coarsening during creep process [24].

The mean diameter size of Laves phase are about 400nm after a long term creep for 113,43 hours at 80 MPa under 600 ° C. The minimum equivalent diameter of Laves phase is 0.7 µm with a magnification of x400 [7]. From the size distribution of Laves phase in P91 steel [7], it can be seen that the Laves phase nucleate at very early stage about 50 hours of creep; it grows until the diameter size of Laves phase of 400nm; then it starts coarsening until fracture with a maximum diameter size of Laves phase about 1400nm [7]. Magnusson [24] also reported the continuously nucleation of Laves phase throughout the creep process, the rate of Laves growth can be determined by assuming a local equilibrium at the particle and matrix interface [24]. Laves phase start coarsening when the growth stage assumed finished which is about 10000 hours at 600 º C [24].

2.1.3 Cavity nucleation, growth and coalescence

Cavity nucleates around large precipitates like Laves phase and $M_{23}C_6$ carbides at grain boundary, growth of cavity due to the nucleation and diffusion of cavities, finally large precipitates coarsening leading to a micro or macro crack [7, 9, 11-12, 21-22, 28, 33]. Dyson [25] has reported two types of cavity evolution. In type one, cavity rapidly nucleate, and then a constant density of grain boundary cavities grow until coalescence at fracture. In type two, cavity nucleation occurs continuously throughout the whole creep lifetime, and then a continuous nucleation and growth of grain boundary cavities until coalescence [25]. Vöse [26] reported that the development of grain boundary cavitation at low stress range is related to the nucleation and diffusive growth of cavities [26]. Therefore, in terms of P91 steel, the grain boundary damage is owing to a continuously cavity nucleation, growth and coalescence of precipitates and cavities.

2.2 Diffusion creep deformation

Diffusion is identified as the creep deformation way at low stress range for high chromium steel grade 91. As it is known, dislocation creep deformation occurs throughout the whole creep process. However, diffusion creep deformation takes the domination at low stress range. The detailed diffusion angles during creep has been reported by Gaffard et al. [27] and also reported by Masse and Lejeail [9, 10]. The Electron Back Scattered Diffraction (EBSD) map shows most of the boundaries rotation angle is $>15^o$ and some of the boundaries rotation angle is $5^o <$ angle $<15^o$. Nabarro-Herring creep is one of the diffusion way. The strain rate of Nabarro-Herring creep is proportional to the stress levels; also the strain rate at the tertiary stage is proportional to the temperature due to its strong temperature dependence.

2.3 Rupture mechanism

The diffusion-assisted brittle rupture is identified as the rupture mechanism at low stress range. The rupture is caused by a large number of cavities nucleation, growth and coaleasence (cavities and participates) at low stress range. The highest number of cavities at fracture surface of creep specimens is about 32, the average diameter size of cavities is about 5.5 μm with a magnification of x400 [7].

2.4 Strain at failure

For P91 steel, the temperature between 600^oC-650^oC is the most common high temperature range. The boundary to distinguish high stress range and low stress range is given in Table 1; according to the investigation on 9Cr-1Mo steel T91 [22].

Table 1: Stress exponent and stress range of transition

Temperature (^oC)	Stress exponent		Stress at change (MPa)
	High stress	Low stress	
500	18.566	3.024	170-210
600	11.929	0.781	70-100
625	10.700	1.729	50-90

Due to the lack of experimental data for P91 steel, 3 sets of data of P91 steel (F. Abe-100MPa-P91 [28]; C.G Panait-80MPa-P91 [6]; K. Sawada-70MPa-P91 [8]) under low stress range at 600^oC are chosen here. The detailed information about these three sets of experimental data is given in Table 2. The different heat-treatment condition could affect the life span of materials, but in here to minimize the error, the experimental data of MGC type at 100 MPa under 600^oC was chosen here to compare with the other two sets of experimental data which is showed in Table 1 at 70Mpa and 80Mpa respectively. By collecting the experimental data from current researches, there are 5 papers (F. Abe-100MPa -P91 [28]; C.G Panait-80MPa-P91 [6]; K. Sawada-70MPa-P91 [8]; Y.F Yin-132MPa-P92 [30]; C. Petry-110MPa-P92 [29]) mentioned the P91/P92 steel under low stress range at 600 ^oC, 3 papers (M.E Abd El-Azim-55Mpa-P91 [31]; T.H Hyde-70Mpa-p91 [3]; Y.F Yin-132MPa-P92 [30];) mentioned the P91/P92 steel under low stress range at 650 ^oC and 1 (T. Masse-60/80MPa-T91[9]) paper mentioned the T91 steel under low stress range at 625 ^oC [3, 6, 8, 9, 24, 29-31].

The relationship between strains at failure and the applied stresses for high chromium steels under different temperatures is shown in Figure 1, based on the previous researches' experimental data [3, 6, 8, 9, 28, 29-31]. At the same temperature condition at 600^oC, the values of strain at failure at 100MPa (MGC type), 80MPa and 70MPa are estimated as 0.0998, 0.0475 and 0.035 respectively [6, 8, 28]. The strain at failure decreases with stress, and approximately, a linear relationship exists. This should be considered in the development of the new set of constitutive equations model. Figure 1shows that the strains at failure at different temperatures within a low stress range are less than 0.1 for high chromium steels.

Besides, NRIM creep data sheet [32] shows the elongation (EL) and reduction of area (RA) of P91 steel tubes at 600^oC under different stress levels. There are no EL and RA when the material ruptured under 100MPa at 600^oC. The values of elongation and reduction of cross-area at 110MPa are 23% and 84%, respectively [33]. However, a stress of 110 MPa at 600^oC is not within the low stress range for P91 steel. At 650^oC, a stress of 70MPa is not within low stress range.

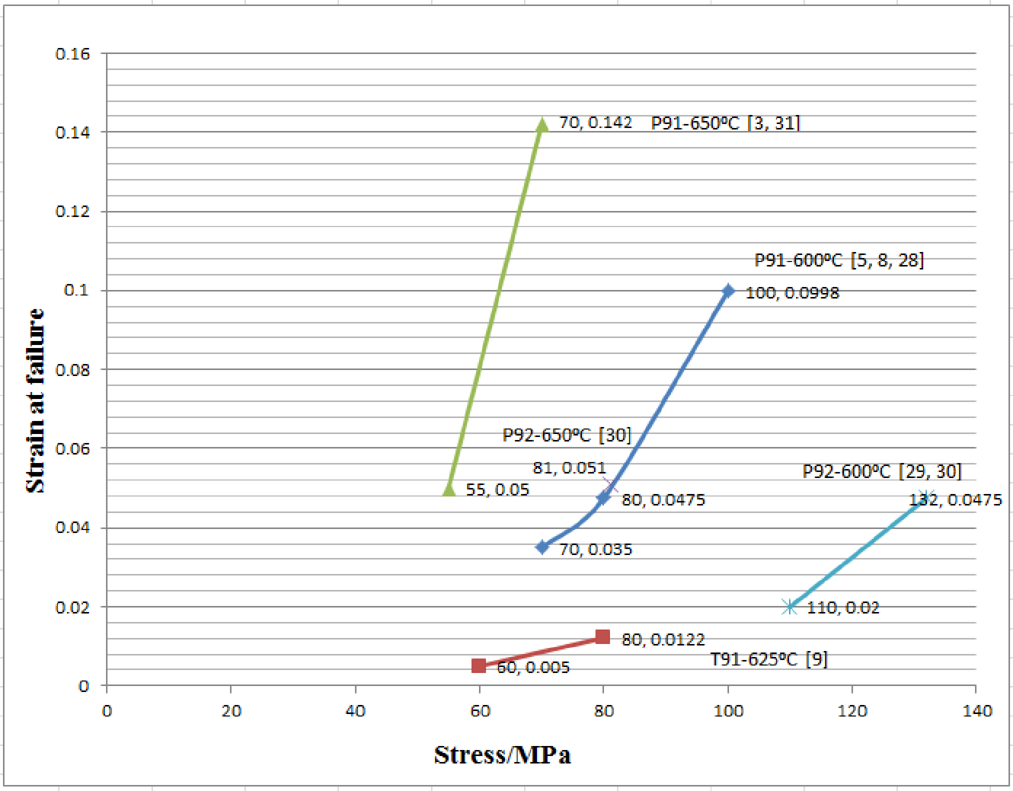

Figure 1: Strain at failure and stress relation for high Cr steels at different temperatures

Table 2: Different heat treatment conditions of P91 tubes

Stress (MPa)	Type	Normalizing	Tempering
100	MGA [28]	1045ºC/10 min AC	780ºC/60 min AC
	MGB [28]	1050ºC/60 min AC	760ºC/60 min AC
	MGC [28]	1050ºC/10 min AC	765ºC/30 min AC
80	Panait [6]	1050ºC/1h/AC	730ºC/1h/AC and 750ºC/1h/AC
70	Sawada [8]	1045ºC/10 min AC	765ºC/30 min AC

2.5 Minimum strain rate vs stresses

For P91 steel, the stress dependence of lifetime is mainly the dependence of the minimum creep strain rate. The relationship between the minimum strain rate and different stresses within low stress range is given in Figure 2. As it is can be seen, the minimum strain rate is linearly proportional to the stresses increasing within the low stress range for high chromium steels at different temperatures [3, 6, 8, 9, 28, 29-31].

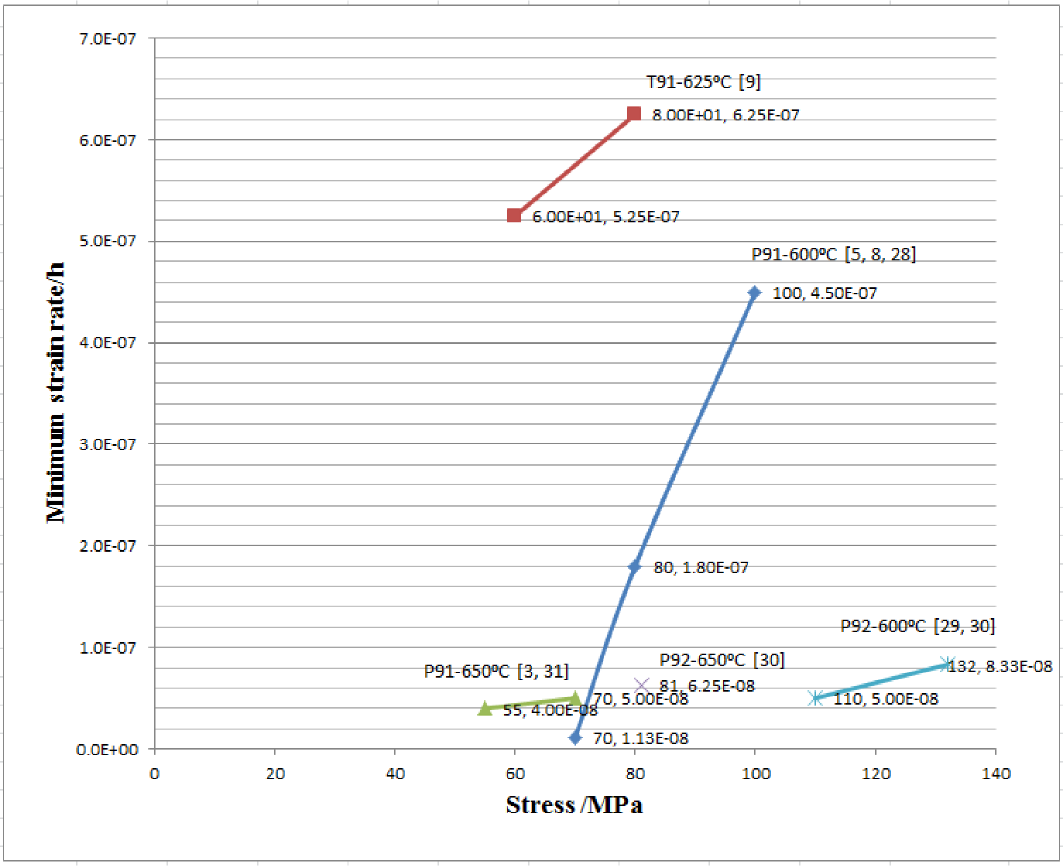

Figure 2: Minimum strain rate and stresses relation for high chromium steels at different temperatures

3 Creep constitutive equations model

3.1 New thoughts for creep damage model

The new thoughts for creep damage model under low stress range will cover the following three aspects: 1) strain at failure is linearly increasing with the stresses; 2) the minimum strain rate is proportional to the stresses; 3) the new failure criterion based on stress and cavitation.

3.2 Constitutive equations model of cavitation

There are many constitutive equations models used for estimating the life span of materials combined with the computational techniques. The most popular models are Dyson's models, Kachanov-Robatnov-Hayhurst models, activation energy models and Norton's law model etcetera.

Now that the creep deformation and rupture mechanisms have been identified in the above section as microstructure changes with diffusion creep process, cavities occurrence and coalescence combined with the applied stress. It has been noted that theoretical models for $M_{23}C_6$, MX type carbides and Laves phase growth and coarsening process and volume fraction of Laves phase exist and they are in such form [34]:

$$d^3 = {d_o}^3 + Kt$$

$$K = K_O \exp[\frac{k\left(\frac{\sigma}{E}\right)^{p_i}}{RT}]$$

$$K_0 = {K_O}' \exp(-\frac{Q_o}{RT})$$

${K_O}'$ and k are two constants, Q_o is activation energy.

The volume fraction of Laves phase (f_{Laves}), which can be decribed in the following equation form for P91 at 600ºC:

$$f_{Laves} = \frac{f_{Laves}^{max}}{[1 + \left(\frac{t}{t_{50,L}}\right)^{-r_L}]}$$

f_{Laves} is the equilibrium fraction at 600ºC, $t_{50,L}$ (=6390 h) is the time for precipitation of 0.5 f_{Laves} and $r_L = 1.85$ according to S. Spigarelli [34]. The parameters for P91 steel at 600ºC are given in the Table 3 [34].

Table 3: Values of parameters for P91 at 600ºC based on paper from S. Spigarelli [34]

Parameters	$K_o(M_{23}C_6)$	$k(M_{23}C_6)$	$p(M_{23}C_6)$	
Values	1.0*10-29	1.8*1011	3.3	
Units	[m³ s-1]			
Parameters	$K_o(MX)$	$k(MX)$	$p(MX)$	
Values	4.0*10-31	7.0*106	1.8	
Units	[m³ s-1]			
Parameters	$K_O(Laves)$	$k(Laves)$	$p(Laves)$	f_{Laves}^{max}
Values	2.7*10-28	3.6*1010	3.5	0.7
Units	[m³ s-1]			[%]

3.3 Stress vs strain rate

From the above information, it is can be identified that the relationship between strain rate and stress is linear relation.

$$\dot{\varepsilon} \propto A\sigma$$

To build the new equation between strain rate and stress, the coupling of microstructure changes, strain at failure, minimum strain rate is the virtual step at the current stage. In addition, the practical applications should be taken to calibrate the new set of constitutive equations.

4 Further work

The form of the new set of constitutive equations model should be determined in the next stage. And then, some applications should be conducted in the further study to validate the new set of constitutive equations model.

References

[1] Shibli A, Starr F. Some aspects of plant and research experience in the use of new high strength martensitic steel P91. Int J Pressure Vessels Piping 2007;84(1):114-122.

[2] TWI holds survey on P91 and P92 grade steel component failures. 2009; Available at: IFM. Accessed 11/14, 2011.

[3] Hyde T, Becker A, Sun W, Williams J. Finite-element creep damage analyses of P91 pipes. Int J Pressure Vessels Piping 2006; 83(11):853-863.

[4] Kimura, K., Kushima, H., & Abe, F. Degradation and assessment of long-term creep strength of high Cr ferritic creep resistant steels. Proc. Inter. Conf. Advances in Life Assessment and Optimization of Fossil Power Plant; 2002.

[5] An LL, Xu Q, Lu ZY, Xu DL. Preliminary analysing of experimental data for the development of high Cr Alloy Creep damage constitutive equations. Automation and Computing (ICAC), 2012 18th International Conference on: IEEE; 2012.

[6] Panait CG, Zielińska-Lipiec A, Koziel T, Czyrska-Filemonowicz A, Gourgues-Lorenzon A, Bendick W. Evolution of dislocation density, size of subgrains and MX-type precipitates in a P91 steel during creep and during thermal ageing at 600 C for more than 100,000 h. Materials Science and Engineering: A 2010;527(16):4062-4069.

[7] Panait C, Bendick W, Fuchsmann A, Gourgues-Lorenzon A, Besson J. Study of the microstructure of the Grade 91 steel after more than 100,000 h of creep exposure at 600 C. Int J Pressure Vessels Piping 2010;87(6):326-335.

[8] Sawada K, Kushima H, Tabuchi M, Kimura K. Microstructural degradation of Gr. 91 steel during creep under low stress. Materials Science and Engineering: A 2011;528(16):5511-5518.

[9] Massé T, Lejeail Y. Creep mechanical behaviour of modified 9Cr1Mo steel weldments: Experimental analysis and modelling. Nucl Eng Des 2013; 254:97-110.

[10] Massé T, Lejeail Y. Creep behaviour and failure modelling of modified 9Cr1Mo steel. Nucl Eng Des 2012; 246:220-232.

[11] Xu Q. Creep damage constitutive equations for multi-axial states of stress for 0.5 Cr0. 5Mo0. 25V ferritic steel at 590° C [J]. Theoretical and applied fracture mechanics, 2001, 36(2): 99-107

[12] Xu Q, Barrans S. The Development of multi-axial creep damage constitutive equations for 0.5 Cr0. 5Mo0. 25V ferritic steel at 590. DEG. C.[J]. JSME International Journal Series A, 2003, 46(1): 51-59

[13] Xu Q. The development of validation methodology of multi-axial creep damage constitutive equations and its application to 0.5 Cr0. 5Mo0. 25V ferritic steel at 590° C [J]. Nuclear engineering and design, 2004, 228(1): 97-106

[14] An LL, Xu Q, Lu ZY, Xu DL. Review of creep deformation and rupture mechanism of p91 alloy for the development of creep damage constitutive equations under low stress level. Proceedings of the 10th international conference on science computing; 2013.

[15] An LL, Xu Q, Lu ZY, Xu DL. Analyzing the Characteristics of the Cavity Nucleation, Growth and Coalescence Mechanism of 9Cr-1Mo-VNb Steel (P91) Steel. Advanced Materials Research 2013; 744:412-416.

[16] Vivier F, Panait C, Gourgues-Lorenzon AF, Besson J. "Creep rupture of a 9Cr1MoNbV steel at 500oC: base metal and welded joint", Nuclear and Engineering Design 2010; 240: 2704-2709

[17] Vivier F, Panait C, Gourgues-Lorenzon AF, Besson J. "Microstructure evolution in base metal and welded joint of Grade 91 martensitic steels after creep at 500-600^{o}C", 17th European Conference on Fracture, Brno, Czech Republic, 2008

[18] Gaffard V, Gourgues-Lorenzon A, Besson J. "Creep failure model of a 9cr1Mo-NbV(P91) steel integrating multiple deformation and damage mechanisms", Ecole des Mines de Paris, Centre des Materiaux, UMR CNRS 7633, BP 87 91003 Evry Cedex France

[19] Besson, J., Leclercq, S., Gaffard, V., & Gourgues-Lorenzon, A. F. Analysis of creep lifetime of a ASME Grade 91 welded pipe. Engineering Fracture Mechanics 2009; 76(10), 1460-1473.

[20] Gupta C, Toda H, Schlacher C, Adachi Y, Mayr P, Sommitsch C, et al. Study of creep cavitation behavior in tempered martensitic steel using synchrotron micro-tomography and serial sectioning techniques. Materials Science and Engineering: A 2013 3/1; 564(0):525-538.

[21] Eggeler G, Ramteke A, Coleman M, Chew B, Peter G, Burblies A, et al. Analysis of creep in a welded 'P91' pressure vessel. Int J Pressure Vessels Piping 1994;60(3):237-257.

[22] Haney EM, Dalle F, Sauzay M, Vincent L, Tournié I, Allais L, et al. Macroscopic results of long-term creep on a modified 9Cr–1Mo steel (T91). Materials Science and Engineering: A 2009; 510:99-103.

[23] Sawada K, Bauer M, Kauffmann F, Mayr P, Klenk A. Microstructural change of 9% Cr-welded joints after long-term creep. Materials Science and Engineering: A 2010; 527(6):1417-1426

[24] Magnusson H, Sandström R. Modelling of the influence of Laves phase on the creep properties in 9% Cr steels[C]//PROCEEDINGS OF THE ASME PRESSURE VESSELS AND PIPING CONFERENCE. 2007: 519-526

[25] Dyson B. Use of CDM in materials modeling and component creep life prediction. Journal of pressure vessel technology 2000; 122(3):281-296.

[26] Vöse M, Otto F, Fedelich B, et al. Micromechanical investigations and modelling of a Copper–Antimony-Alloy under creep conditions[J]. Mechanics of Materials, 2014, 69(1): 41-62.

[27] Gaffard V, Gourgues-Lorenzon A, Besson J. High temperature creep flow and damage properties of 9Cr1MoNbV steels: Base metal and weldment. Nucl Eng Des 2005; 235(24):2547-2562

[28] Abe F. Creep modeling and creep life estimation of Gr. 91. International journal of materials research 2012;103(6):765-773.

[29] Petry C, Lindet G. Modelling creep behaviour and failure of 9Cr–0.5 Mo–1.8 W–VNb steel. Int J Pressure Vessels Piping 2009; 86(8):486-494.

[30] Yin, Y. F., & Faulkner, R. G. Continuum damage mechanics modelling based on simulations of microstructural evolution kinetics. Materials science and technology 2006; 22(8): 929-936.

[31] Abd El-Azim M E, Ibrahim O H, El-Desoky O E. Long term creep behaviour of welded joints of P91 steel at 650° C [J]. Materials Science and Engineering: A 2012; 560:678-684.

[32] NRIM Materials Database: National research institute for material. 1996;43.

[33] Shrestha T, Basirat M, Charit I, Potirniche GP, Rink KK. Creep rupture behavior of Grade 91 steel. Materials Science and Engineering: A 2013.

[34] Spigarelli S. Microstructure-based assessment of creep rupture strength in 9 Cr steels. Int J Pressure Vessels Piping 2012